

HORTICULTURAL SENSING BY PHOTOACOUSTICS AND THERMAL LENSING

Dane Bicanic¹, Paul Torfs², Marcel Lubbers³ and Andrew Tam⁴

- 1 Laser Photoacoustic Laboratory, Department of Agricultural Engineering and Physics, Wageningen, Agricultural University, Duivendaal 1, 6701 AP Wageningen, The Netherlands
- 2 Department of Hydrology, Soil Physics and Hydraulics, Agricultural University, Nieuwe Kanaal 11, 6709 PA Wageningen, The Netherlands
- 3 Department of Soil Science and Geology Wageningen, Agricultural University, Duivendaal 10 6700 AA Wageningen, The Netherlands
- 4 IBM Research Division, Almaden Research Center 650 Harry Road, San Jose, California 95120, USA

Abstract

Principles of photoacoustic and photothermal trace detection in gas and liquid phase are being discussed. Recently obtained results that are of interest in the horticultural and the environmental sector are presented.

1. Introduction

Steadily growing public concern about our environment requires the experimental techniques and the equipment capable of selective and sensitive trace detection, i.e. measuring minute quantities of certain material substance in the presence of other constituents. The same is true for many other areas of research and practice. During the last decade class of photothermal spectroscopies has emerged as the prospective candidate technique. Contrary to other methods, it can be applied to all sort of samples and provides in addition, considerable selectivity and respectable detection limits (although inferior to ultrasensitive methods detecting quantum effects) at the reasonable cost without a need for tedious preparation of the sample. Consequently large number of data reporting the results of photothermal studies on a variety of samples in all three phases has appeared in the scientific literature. It is now established that photothermal spectroscopies enable the optical and the thermal characterization of weakly absorbing (i.e. highly transparent) as well as of the completely opaque and scattering samples.

This paper makes no attempt to discuss the subject of photothermal science in extenso. The topic has become a very active field of research, both experimental and theoretical, and is being well documented in a few excellent reviews and text books (Tam 1986, Sell 1988, Hess 1989, Mandelis 1991). However despite such intensive developments and the progress achieved, little photothermal equipment has been incorporated in the analytical instrumentation so far, and the technique is still unknown to a wide range of potential users. It is for this very reason that basic underlying principles behind the physics of photothermal methods will be presented here. Special emphasis is placed on the two methods: the photoacoustic detection and the photorefractive techniques (such as collinear photothermal deflection and the thermal lensing) that have proven very valuable tool in concentration measurements of atmospheric pollutants and of

inorganic constituents dissolved in the water and in the soil water solutions.

The photothermal spectroscopies share one common thing: they all deal with detection of thermal effects induced in the sample, on the sample or in the medium surrounding the sample of interest. These macroscopic effects are however a direct consequence of the heating generated by the absorption of incident radiation. The irradiated sample relaxes dominantly by collisions releasing thereby the absorbed energy; the effect that results in an increase of the sample's thermal energy. The oldest and perhaps the most explored photothermal method is the photoacoustic (PA) detection where the periodically interrupted radiation emitted by the source L (power P) causes the corresponding periodic heating and cooling of the specimen (for example gas) enclosed in the measuring chamber M of a fixed volume (called PA cell). This leads to the generation of the pressure wave, i.e. sound in the cell that is being detected by the suitable transducer such as micro-phone whenever the emission frequency of the source and the absorption frequency of the sample coincide. The basic difference between the PA and other traditional spectroscopies is in the way by which the power P_{abs} absorbed by the sample is being detected as shown in Fig. 1a and 1b.

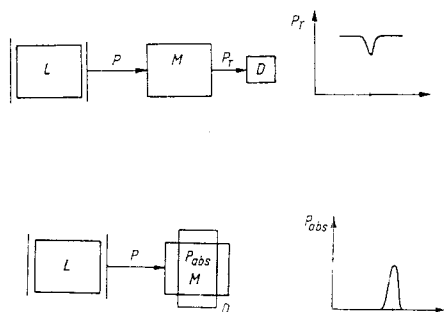


Figure 1a - Traditional transmission spectroscopy.

Figure 1b - Photoacoustic and photothermal methods are zero-background techniques. Signal is generated only when there is an absorption.

The conventional methods (Fig. 1a) imply two independent measurements, i.e. the transmitted power P_{tr} monitored with the detector D (or reflected and scattered power) is compared to the incident power P and the information about the sample's absorbance is derived a relevant difference. The presence of absorption is evident by a dip in the transmission spectrum. For the weakly absorbing samples it becomes difficult to measure accurately the small difference between two almost practically equal signals and the experimental error increases drastically. Fractional absorption of 10^{-3} is currently thought as detection limit of traditional spectroscopies.

In photoacoustics the power deposited in the sample is measured directly and therefore there exists no need for two independent measurements. For a given geometry of the PA cell the amount of power absorbed P_{abs} is directly proportional to the concentration C of the absorbing sample, to the sample's absorption coefficient α (being

proportional to the trace gas partial pressure) at the given emission wavelength and to the incident power P . Hence it is in the principle possible to translate otherwise weak absorbance ($\alpha \ll 1$) into the measurable sound signals if substantial incident power P is available. The PA is essentially a zero-background technique meaning that the PA signal will only be generated if there is an absorption (Fig. 1b). The fractional absorption as low as 10^{-9} to 10^{-10} have been achieved with the strongly absorbing gases (classified as atmospheric pollutants) and powerful infrared lasers in the combination with sophisticated signal processing techniques. In general, in case of trace detection which is equivalent to a weak absorption, the magnitude S of the electric signal detected by the microphone is directly proportional to the product $P \propto C$. The proportionality constant R , called the cell responsivity does include the geometrical and design parameters, the sensitivity of the microphone and the "acoustic quality factor" of the cell. Its value is determined by the calibration using the test gas. Two modes of operation are possible. In the analyzing mode, while scanning the wavelength of the source, one measures the normalized signals (S/P) obtained from a given gaseous constituent of precisely known concentration C and uses the relationship $\alpha = S/(RPC)$ to record the spectral fingerprint for molecule of interest. When however the absorption coefficients α are known it is possible to operate photoacoustic spectrometer in the monitoring mode by recording the normalized signals (S/P) to determine C . In the multicomponent mixtures the unknown concentrations are recovered from the set of linear equations taking in account both, the signal and the phase of the measured PA signals. Selectivity can be improved by working at low pressures instead at the atmospheric (to reduce the linewidth of the absorption line and hence also the spectral overlap) but at the expense of loss in the signal magnitude. Other, more complex experimental schemes (such as for example the application of the external electric field whenever dealing with the molecules having the permanent dipole moment) can also be used in order to suppress unwanted spectral interferences.

It is clear that some degree of spectral coincidence between the emission wavelength of the source and the wavelength at which the gas absorbs is an impetus for the efficient PA measurement. No continuous source of high power is however available in the infrared region where many gaseous molecules of interest possess their specific and strong absorption transitions. The step-tunable tunable carbondioxide (emission range 9-11 microns) and the carbon monoxide (emission range 5-7 microns) lasers provide high output powers and have been used intensively to collect the library of data. On the other hand solid state diode lasers are virtually continuously tunable in the infrared region of the electromagnetic spectrum but their power output lasers are several orders of magnitude below these provided by the carbondioxide laser. Having the strong radiation of a desired wavelength it is a matter of a major concern to design an efficient PA cell. This implies the optimization of the acoustic signal while minimizing simultaneously the noise. For vibrationally isolated PA cell and the low noise modulator, the main cause of the noise is not electronics but instead the heating (due to the absorption of radiation in the windows used to seal the PA cell from the ambient) and warming effects caused by reflected and scattered radiation. Both of these processes do generate the heat and since this latter is being modulated

at the same frequency as a desired signal, the electronic processing unit will detect these unwanted "background" signals. As far as design of the PA cell is concerned two basic approaches are being employed. The resonant PA cell acts as an acoustic amplifier (with a quality factor $Q > 1$) when the modulation frequency corresponds to one of the cell's acoustic resonances determined by the cell geometry, dimensions and gas dependent velocity. These conditions impose restrictions regarding the cell volume. On the other hand the non-resonant cell has a quality factor equal to unity, but it can be made small which is of interest in particular when fast, real-time measurements in the flow mode are being concerned.

Most of the practical gas phase PA experiments were carried out in the environmental sector. Widespread research programs are underway the main aim being the construction of a reliable, sensitive and fast PA concentration detector for monitoring several atmospheric constituents (in the presence of other interfering gases) capable of unattended operation over prolonged intervals of time. Large number of gases in the non-absorbing nitrogen were investigated in the laboratory under well controlled conditions in order to determine their spectral fingerprint. The spectral region between 9 and 11 microns is the most intensely explored due to the versatility of the CO_2 laser. The air-pollution mobile monitoring unit at Swiss Federal Institute of Technology has been applied to immission studies in the urban areas, analysis of automobile and industrial exhausts (Meyer and Sigrist 1990) including detection of ethylene as well as of other hydrocarbons, water vapour, carbondioxide, vinylchloride, alcohols, dichlormethane, toluene, xylenes and many others. Photoacoustic studies of gases of agricultural interest including ozone, hydrogen sulphide, 1,2 dibromethane and ethylacetate have been performed (Harren et al. 1990) and detection limit of 20 ppt for ethylene in the realistic air samples has been achieved. Detection of ammonia is (due to its role in the acidification of soil) nowadays of great importance and has been attracting the attention of PA investigators. Although ammonia has large absorption coefficient in the CO_2 laser region, PA concentration measurements in the near ppb range are seriously hampered by the interference due to the water and carbondioxide (that causes "kinetic cooling" effect). Correct interpretation of ammonia concentration measurements has been done (Roth et al. 1990) using the PA amplitude and phase data obtained at two laser lines. The approach that involves the use of only one laser transition, yet enabling the few ppb on line detection limit is that of Stark spectroscopy (Sauren et al. 1989, Sauren et al. 1990) based on application of the external electric field to the gaseous mixtures under investigation. Recent cross-interference studies (Sauren et al. 1991) aimed to detect various levels of ammonia in water vapour and carbondioxide mixtures have provided final evidence about the usability of such approach. Diurnal variation of ammonia concentration (near ppm range) in the hot smokestack emission has been investigated too (Olafsson 1990, Henningsen et al. 1990). Important is also the PA detection of ammonia rates emitted from different depths of the fertilized soil and the ammonia flux measurements (Artemov et al. 1986). The prospects of the CO_2 laser for monitoring the N_2O gas as a tracer used in the ventilation rate measurements in the greenhouse has been investigated (Bićanic et al. 1988). Detection limit of 1 ppm can be pushed back by using the CO laser because of more favourable absorption coefficient of N_2O . Study on the complex molecules such as

potato sprouting suppressants carvone and pulegone showed (Bicanic et al. 1990a) that 2 ppm can be reached at CO₂ laser wavelengths compared to 35 ppb in the wavelength range covered by the CO laser emission. Larger molecules such as 1,3 dichloroethane, dichlorvos and malathion pesticides exhibit (Bicanic et al. 1989) "featureless, gaslike" spectra between 9 and 11 microns but distinction between cis and trans isomers could be made. Perhaps the best example of the applicability of the laser based photoacoustics is the monitoring of ethylene, a gaseous hormone, as the indicator of stress in ornamental flowers. After the initial work (Woltering et al. 1988) on the ethylene production rates of emasculated ornamental flowers, large diversity of studies followed (Woltering 1990) including these on the inundated plants (Harren 1988). Several manufacturers brought the PA detectors on the market in the recent years these however incorporate thermal sources emitting moderate power levels; nevertheless excellent detection limits are being claimed for several atmospheric gases. Compact carbon dioxide gas monitors for operation in the steady state and in the flow mode are available. The PA analyzer capable of measuring the CO₂ and H₂O exchange of a photosynthesizing leaf was recently suggested and tested in practice (Oehler and Blum 1990). A biosensor (urease immobilized on glass beads) based on the PA detection of gases produced by an enzyme was developed (Oehler et al. 1985). Novelty is also the solid state sensor (PVDF) pyroelectric foil sputter-coated with Pd that was used (Mandelis and Christofides 1991) to detect the concentrations of hydrogen as small as 0.075 % in a flowing mixture of H₂+N₂ mixtures. The same foil was used in a different technique to observe the instant of condensation of water vapor in the atmosphere (Chirtoc et al. 1991). Methane is another gas of practical interest and due to the perfect coincidence between the emission line of infrared He-Ne laser (3.39 microns) and the strong absorption line of methane near ppb detection limit can be anticipated. With the improvements in the laser technology and that of electronics being far from exhausted, further progress can be expected in the immediate future.

2. Material and methods

The peculiar properties of the laser radiation form the basis for the use of photothermal (PT) refraction techniques. Although the principles do apply equally well to all aggregate states, in this paper attention is paid to the liquid phase since our experiments were done with either pure liquids or the aqueous solutions. Consider the Cartesian coordinate system in Fig. 2a.

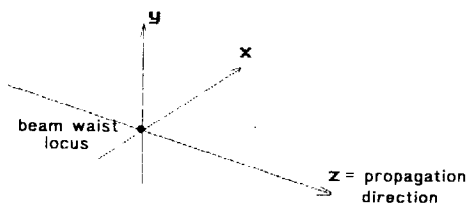


Figure 2a - The coordinate system indicating location of the beam waist and the propagation direction.

The collimated radiation beam (unfocussed diameter d_0) originating from the laser source (wavelength and power P) propagates in a direction of z -axis and passes through the converging lens (focal length F_1). For the laser operating in the TEM_{00} mode the beam intensity profile $I(x,y,z)$ is the Gaussian displayed in Fig. 2b (for a constant z value) and given by:

$$I(x,y,z) = [2P/\omega^2(z)\pi] \exp \{-2[(x^2 + y^2)/\omega^2(z)]\} \quad (1)$$

where

$$\omega(z) = \omega_0 (1 + [z/z_c]^2) \quad (2)$$

is the radius of the beam and z_c is the confocal distance defined as $z_c = \pi\omega_0/\lambda$. The parameter ω_0 is the beam waist, i.e. the radius of the laser beam in the focus of the lens, and can be chosen at will since $\omega_0 = (\lambda F_1/\pi d_0)$. The location of the beam waist in Fig. 1a d_0 is at the origin of the coordinate system (for $z=0$ it follows $\omega(0) = \omega_0$ from eqn.2). It is clear that the spot size increases with a distance from the waist (Fig. 2c); hence the Gaussian profile

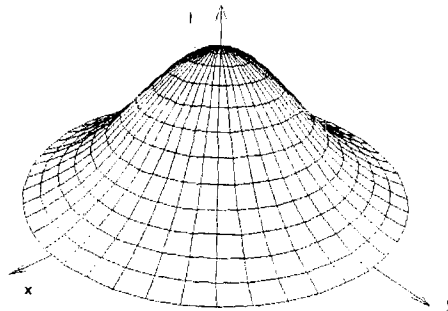


Figure 2b The Gaussian intensity distribution $I(x,y,z)$ given by eqn. 1 is symmetrical with respect to the propagation direction (z axis)

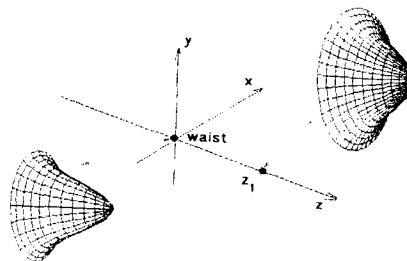


Figure 2c The spatial form of the laser beam at $z=0$ and at $z=z_1$.

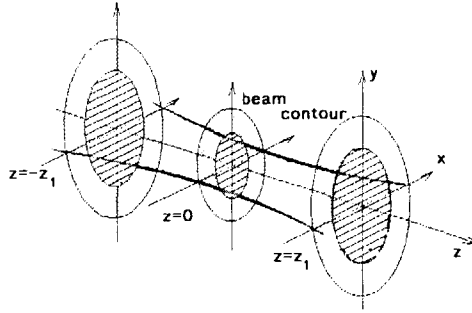


Figure 2d Distribution of laser beam intensity at three values of z . The shaded regions correspond to a distance equaling single and double size of the beam waist.

is spread more widely but the total volume remains constant. The physical meaning of the beam waist is illustrated in Fig. 2d; for a given z 86 % of the total beam intensity is concentrated within the circle having radius being equal to ω compared to 99.9 % within the radius of 2ω (as indicated by the beam contour and the shaded regions for three planes located at $z=-z_1, z=0$ and $z=z_1$ respectively. The $x-z$ plane cut with the corresponding regions is shown in Fig. 2e.

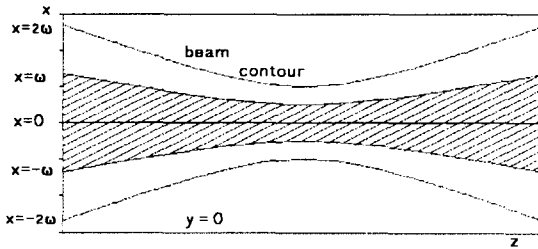


Figure 2e The beam contour in the $x-z$ plane.

Assume now sinusoidally modulated laser beam (modulation frequency Ω) incident on the homogenous liquid (density d and the specific heat at the constant pressure c_p) containing the species with the absorption coefficient β (cm^{-1}) at the laser wavelength. Due to the absorption of the laser power in the sample along the z -axis, the temporal and spatial variation of the intensity is given by the eqn.1 multiplied by the factor $(1/2)(1+\cos \Omega t) \exp(-\beta z)$. The heat source $Q(x,y,z,t)$ is being generated in absorbing sample since $Q(x,y,z,t) = -\beta I(x,y,z,t)$. The temperature profile $T(x,y,z,t)$ resembles that of $I(x,y,z,t)$ and the time rate change T of the temperature can be calculated from $T(x,y,z,t) = (\beta/dc_p) I(x,y,z,t)$. Liquids, when heated experience the change in the refractive index n and for most liquids temperature coefficient dT/dn is negative. Since the temperature in the sample varies, the refractive index becomes place dependent too and hence the heated sample acts as an divergent thermal lens. Contrary to its optical counterpart, thermal lens needs a certain amount of time to be created. This latter is for a given species determined by the amount of power deposited (i.e. the incident power P and the beam waist ω_0) in

the sample and material and thermal properties of the bulk liquid that influence the dissipation of the lens. Thermal lens is the strongest at places corresponding to a maximum of the temperature gradient ($\partial T/\partial \rho$). Inspection of the temperature profile $T(x,y,z)$ displayed in

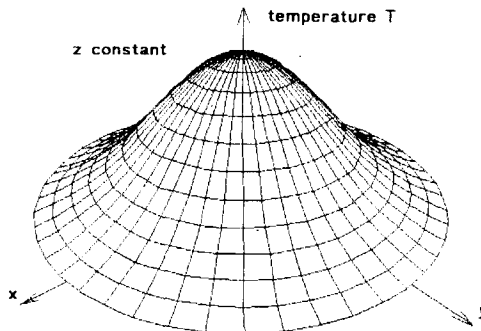


Figure 2f Laser induced temperature profile in the uniformly absorbing liquid.

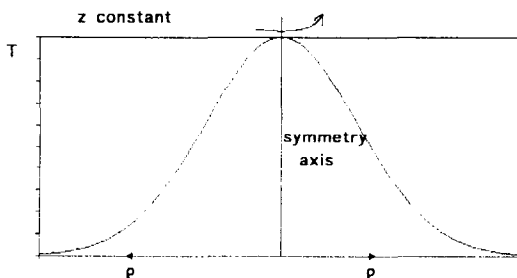


Figure 2g Temperature profile T versus ρ at the constant z value.

Fig. 2f leads for a given z , to the two dimensional (T, ρ) contour $\rho = (x^2 + y^2)^{1/2}$ that is symmetric with respect to the z -axis (Fig. 2g). Likewise the temperature gradient $\partial T/\partial \rho$ shown in Fig. 2h is also symmetric with respect to $\rho = 0$ and exhibits two equally strong maxima (for z is constant) located at distance corresponding to $\omega/2$. This result is obtained by differentiating (with respect to ρ) the expression for $T(x,y,z,t)$. Rotating the contour in Fig. 2h about the symmetry (z) axis provides a three dimensional plot of the temperature gradient $\partial T/\partial \rho$ displayed in Fig. 2i.

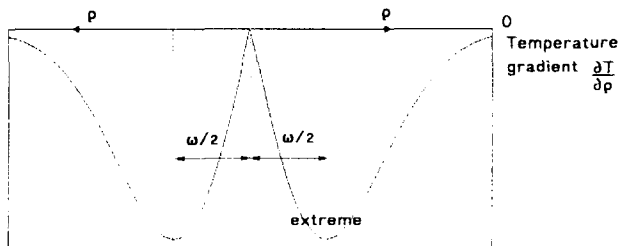


Figure 2h The temperature gradient at the constant z . The working of the lens is strongest at the points of maxima distributed symmetrically with respect to the z axis.

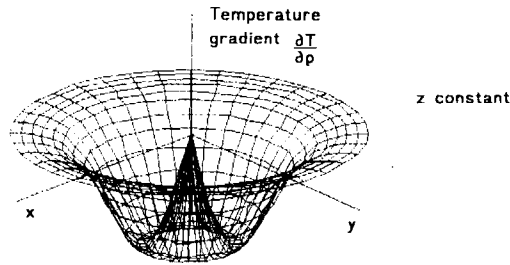


Figure 2i The 3-dimensional plot of the thermal gradient at the given z .

All pairs of (x,y) points satisfying the relationship $\rho = (x^2 + y^2)^{1/2} = \omega/2$ form the circle along which the strength of the lens is maximal. Exactly on the beam axis the temperature gradient vanishes. Finally, as one moves away from the beam waist ($z=0$) to $z_1 > 0$ the plot $\partial T/\partial \rho$ changes in the way shown in Fig. 2j. The fact

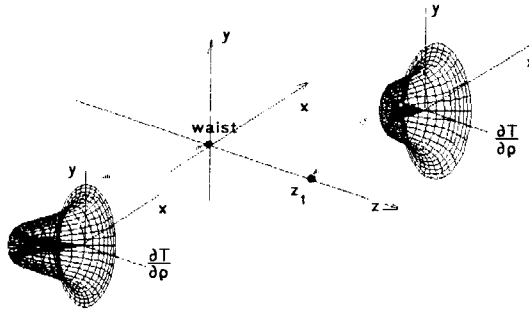


Figure 2j The variation of the thermal lens with the distance from the beam waist.

that $\partial T/\partial \rho$ is directly proportional to the absorption coefficient β (per unit length) of the sample can be conveniently used to construct the concentration monitor since β is proportional to C . In practice the intensity modulated laser, called the "pump" is used to induce the heating in the sample. The generated thermal lens is then being "scanned" by another, "probe" laser the radiation of which is not absorbed by the sample. When the probe beam traverses the location of maximum temperature gradient, it will be periodically deflected (at the modulation frequency of the pump laser) due to the varying refractive index gradient. Figure 3 shows the experimental arrangement used in our experiments. The pump beam PuB modulated at Ω is focused by the lens L1 into the standard cuvette C (length L) carrying the liquid sample (refractive index n_0 , the temperature coefficient dn/dT). The probe beam PrB is focussed by the lens L2 to form a spot in the middle of the cuvette. The diameter of the probe beam is about six times smaller than that of the pump beam. The two beams intersect each other at an angle of approximately 3 degrees. Detail drawing displays the induced temperature and the temperature gradient in the $z=0$ plane. A deflection angle ϕ is measured as the electric signal S obtained at the modulation frequency from the quadrant or lateral position sensitive

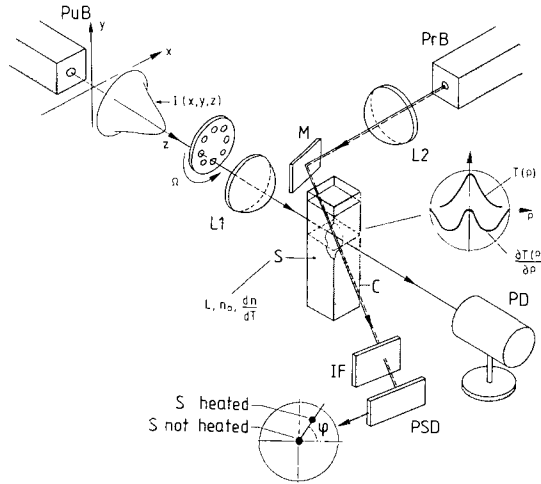


Figure 3. The collinear photothermal deflection experiment used in this study. The meaning of all the symbols is given in the text.

detector PSD in the combination with the lock-in amplifier. When no heating is involved, there is no deflection and the spot of the probe beam at the PSD detector is equally distributed across the four quadrants giving $S=0$. It has been established that for weakly absorbing solutions the magnitude of the signal S is given by

$$S \sim - F (L/n_0) (dn/dT) (\beta/d c_p) (4 \rho/\omega^2) I(x,y,z,t) \quad (3)$$

where F denotes the detector's transducer factor (typically 10^3 V/rad) $(1/n_0)(dn/dT)$ is the relative change of the index of refraction with the temperature and L is the interaction length between the two beams. The method by which the refractive index gradient is probed in the way described above is termed the collinear photothermal deflection contrary to the orthogonal configuration also named mirage. The amount of sample's absorption can be determined by another photorefractive technique called thermal lensing. It has been shown that the absorbing sample acts as the divergent lens affecting the pump beam. Therefore there is a change in the intensity of the pump beam along its axis. This change can be easily observed by placing a detector behind the pinhole the axis of which coincides in space with that of the pump beam. Other thermal lensing experimental schemes that involve the use of both the probe and the pump beam are often used and the relevant mathematical expressions can be found in the literature.

3. Results

The primary aim in our experiments was to investigate the potential of the photorefractive methods for low level detection of ammonium, orthophosphate, pyrophosphate and bentazone all dissolved in the water and to compare the results to those available with the commercial equipment. The knowledge about orthophosphate and ammonium concentrations is of interest in the soil science and horticulture. On the other hand the inorganic pyrophosphate plays the very important metabolic role in potato chemistry. Finally bentazone is the toxic

constituent that was shown to threaten drinking water power supplies and its concentration levels must be controlled.

Water, the biological fluid, exhibits low absorption in the visible part of the spectrum, but becomes opaque at infrared wavelengths. Unfortunately, all the above mentioned solutes, with the exception of bentazone, have their characteristic absorption band in the infrared. To achieve the needed spectral coincidence colorimetric complexes absorbing in the visible must be formed. Inexpensive He-Ne laser (emitting 7 mW of power at 633 nm) and the miniature semiconductor GaAlAs laser (emitting 4 mW at 790 nm) were used here. The indophenol complex formed by the indophenol blue colorimetry has an absorption band centered between 600 and 700 nm with the maximum near 640 nm. Detection limit better than 0.25 mmole/m³ for ammonium in water has been achieved (Strauss et al. 1991). In case of orthophosphate the detection limit of 0.1 mmole/m³ was obtained using the molybdenum blue colorimetry and the GaAlAs laser as the pump (Bicanic et al. 1990b). Both values are superior to these offered by the transmission methods. The same is true for the pyrophosphate in extracts of potato tubers where detection limit of 0.14 microgram/3.7 ml could be reached using the set-up for nearly collinear photothermal deflection experiments (Bicanic et al. 1991). For bentazone not more than 10 ppm could be detected using the methylene blue colorimetry (Schlangen et al. 1991) but the availability of UV source would push the detection limit into a subppb range. The instrumentation used in our experiments is basically very simple and constructed from the readily available and inexpensive components.

4. Conclusion

Detection limits reported above are not restricted by the noise but instead by the absorption of the solvent itself. Further sensitivity enhancement can easily be accomplished by the differential measurements. Among these, dual beam and dual wavelength thermal lensing (Franko and Tran 1988) or detection of second harmonic of the modulated thermal lens (Pang and Morris 1984) present probably the best solution. In conclusion, present state of technological development of lasers will undoubtedly lead to the full realization of the potential different photothermal methods have for highly sensitive and selective sensing in the gaseous, liquid and solid phase.

Acknowledgments

The authors thank to Ms. Dos L'Ami from the local University for taking care of the final manuscript.

References

- Artemov, V., Zharov, V., 1987. Detection of ammonia from fertilized fields. Proc. 5th International Meeting on Photoacoustic, Photothermal and Related Phenomena, Heidelberg 1987.
- Bicanic, D., Bizzarri, A., Zuidberg, F., Bot, G., de Jong, T. Wegh, H., 1988. Carbondioxide laser based monitor of nitrous oxide. In: Photoacoustic and Photothermal Phenomena (P. Hess and J. Pelzl eds.). Springer Series in Optical Sciences 58: 143-146. Springer Verlag Berlin.

- Bicanic, D., Jalink, H., Sauren, H., 1989. Photoacoustic investigation of pesticides. In: *Monitoring of Gaseous Pollutants by Tunable Diode Lasers* (R.Grisar ed.) 280-288. Kluwer Academic Publishers Dordrecht.
- Bicanic, D., Zuidberg, B., Jalink, H., Miklos, A., Hartmans, K., van Es, A., 1990a. The assessment of laser photoacoustic spectroscopy as the analytical tool for studying the potato supressants carvone and pulegone. *Appl. Spectr.* 44: 263-266.
- Bicanic, D., Favier, J.P., Strauss, E., Lubbers, M., Fleuren, G., 1990b. Low cost colorimetric measurement of phosphate trace levels in water and in soil solutions by the collinear photothermal beam deflection method. *Inter.Jour. Environ. Anal.Chem.* 38:623-628.
- Bicanic, D., Favier, J.P., Miklos, A., de Ruiter H., 1991. Comparison between the enzymatic and photorefractive technique in detecting the inorganic pyrophosphate in extracts of potato tubers. *Agrochimica* (submitted).
- Chirtoc, M., Bicanic, D., Tosa, V., 1991. Versatile IPPE technique and instrument for real time observation of the condensation of water vapour in the atmosphere. *Rev.Scie. Instrum.* (submitted).
- Franko, M., Tran, C., 1988. Development of a double-beam, double wavelength thermal lens pectrometer or simultaneous measurement of absorption at two different wavelengths. *Anal. Chem.* 60: 1925-1928.
- Harren, F., 1988. Photoacoustics-refined and applied to biological systems. Ph.D. Thesis. Catholic University Nijmegen.
- Harren, F., Reuss, J., Woltering, E., Bicanic, D., 1990. Photoacoustic measurements of agriculturally interesting gases and detection of ethylene below the ppb level. *Appl. Spectr.*44:1360-1368.
- Henningsen, J., Olafsson, A., Hammerich, M., 1990. Trace gas detection with infrared gas lasers. In: *Applied Laser Spectroscopy*, M.Inguscio and W. Demtroder (Eds.), Plenum ASI (in press).
- Hess, P., 1989. Photoacoustic, photothermal and photochemical processes in gases. *Topics in Current Physics* 47. Springer Verlag Berlin.
- Mandelis, A., 1991. Progress and perspectives of photothermal and photoacoustic phenomena. Elsevier Science Publishers, New York (in press).
- Mandelis, A., Christofides, C., 1991. Photopyroelectric (P₂E) sensor for trace hydrogen detection. *Sensors and Actutors* (submitted).
- Meyer, P., Sigrüst, M. W., 1990. Atmospheric pollution monitoring using carbondioxide laser photoacoustic spectroscopy and other techniques. *Rev. Scien. Instrum.* 61: 1779-1907.
- Oehler, O., Seifert, M., Cliffe, S., Mosbach, K., 1985. Detection of gases produced by biological systems with an enzym photoacoustic sensor. *Infrared Phys.* 25: 319-321.
- Oehler, O., Blum, H., 1990. Photoacoustic measurement of plant gas exchange. In: *Photoacoustic and Photothermal Phenomena II.* (J. Murphy ed.). Springer Series in Optical Sciences 62: 369-371. Springer Verlag Berlin.
- Olafsson, A., 1990. Photoacoustic molecular spectroscopy with tunable waveguide carbondioxide lasers. Ph.D. Thesis. University of Copenhagen.
- Pang, T., Morris, M., 1984. Liquid chromatography detection at the second harmonic of the modulated thermal lens. *Anal. Chem.* 56: 1467-1469.
- Roth, R., Verhage, A., Wouters, L., 1990. Photoacoustic measurements of ammonia in the atmosphere. *Appl.Optics* 29:3643-3653.
- Sauren, H., Bicanic, D., Hillen, W., Jalink, H., van Asselt, K., Quist J., Reuss, J., 1990. Resonant Stark spectrophone as an enhanced